Signal Transducer and Activator of Transcription 3 Is Required for Myocardial Capillary Growth, Control of Interstitial Matrix Deposition, and Heart Protection From Ischemic Injury

Denise Hilfiker-Kleiner, Andres Hilfiker, Martin Fuchs, Karol Kaminski, Arnd Schaefer, Bernhard Schieffer, Anja Hillmer, Andreas Schmiedl, Zhaoping Ding, Edith Podewski, Eva Podewski, Valeria Poli, Michael D. Schneider, Rainer Schulz, Joon-Keun Park, Kai C. Wollert, Helmut Drexler

Abstract—The transcription factor signal transducer and activator of transcription 3 (STAT3) participates in a wide variety of physiological processes and directs seemingly contradictory responses such as proliferation and apoptosis. To elucidate its role in the heart, we generated mice harboring a cardiomyocyte-restricted knockout of STAT3 using Cre/loxP–mediated recombination. STAT3-deficient mice developed reduced myocardial capillary density and increased interstitial fibrosis within the first 4 postnatal months, followed by dilated cardiomyopathy with impaired cardiac function and premature death. Conditioned medium from STAT3-deficient cardiomyocytes inhibited endothelial cell proliferation and increased fibroblast proliferation, suggesting the presence of paracrine factors attenuating angiogenesis and promoting fibrosis in vitro. STAT3-deficient mice showed enhanced susceptibility to myocardial ischemia/reperfusion injury and infarction with increased cardiac apoptosis, increased infarct sizes, and reduced cardiac function and survival. Our study establishes a novel role for STAT3 in controlling paracrine circuits in the heart essential for postnatal capillary vasculature maintenance, interstitial matrix deposition balance, and protection from ischemic injury and heart failure. **(*Circ Res*. 2004;95:187-195.)**

Key Words: mouse ■ signal transduction ■ angiogenesis ■ ischemia ■ heart failure

Activation of signal transducer and activator of transcription 3 (STAT3) in the heart has been observed in acute myocardial infarction (MI), ischemic preconditioning, and pressure overload.[1–3] In this regard, activation of the stress-responsive Janus kinase (JAK)–STAT signaling pathway during ischemia/reperfusion (I/R) injury and MI has been proposed to provide protection against ischemic stress via transcriptional activation of cytoprotective genes.[1,4] Cell culture studies have ascribed some of the cytoprotective actions of the JAK–STAT pathway in cardiomyocytes specifically to STAT3 activation.[5] However, although STAT3 activation is clearly associated with an upregulation of a wide array of target genes in cardiomyocytes, it is unclear which of the reported cardiac responses associated with STAT3 activation are indeed required in vivo for controlling cardiac growth, function, tissue architecture, or protection against cardiovascular stress such as ischemic injury. Importantly, although increased circulating levels of interleukin **(**IL)-6–related cytokines predict mortality in patients with heart failure and may enhance gp130 activation in the failing human heart, expression and phosphorylation levels of STAT3 are severely depressed in myocardium obtained from patients with dilated cardiomyopathy,[6] raising the possibility that decreased STAT3 activation may contribute to development of cardiac failure in patients.

To elucidate the potential role of STAT3 in cardiac muscle and, in particular, for cardiac protection against physiological and pathophysiological stress, we created mice with a cardiomyocyte-restricted STAT3 deletion.

Materials and Methods

Cardiomyocyte-Specific STAT3 Deletion

STAT3-floxed mice[7] and α-myosin heavy chain (αMHC)-promoter/Cre-recombinase transgenic mice[8] were bred to generate mice with a cardiomyocyte-restricted STAT3 deletion (online data supplement available at http://circres.ahajournals.org). Only male mice were studied. All animal studies were in compliance with the *Guide for the Care and Use of Laboratory Animals* as published by the US

Original received December 22, 2003; revision received May 26, 2004; accepted May 27, 2004.

From the Departments of Cardiology and Angiology (D.H.-K., A. Hilfiker, M.F., K.K., A. Schaefer, B.S., A. Hillmer, Edith Podewski, Eva Podewski, K.C.W., H.D.), Anatomy (A. Schmiedl), and Nephrology (J.-K.P.), Medical School Hannover, Germany; Institute for Cardiovascular Physiology (Z.D.), University of Düsseldorf, Germany; Department of Genetics, Biology, and Biochemistry (V.P.), University of Turin, Italy; Department of Medicine (M.D.S.), Baylor College of Medicine, Houston, Tex; Department of Pathophysiology (R.S.), Universitätsklinikum, Essen, Germany.

Correspondence to Helmut Drexler, MD, Abt Kardiologie und Angiologie, Medizinische Hochschule Hannover, Carl-Neuberg Str 1, 30625 Hannover, Germany. E-mail drexler.helmut@mh-hannover.de

National Institutes of Health and approved by our local institutional review boards.

Animal Experiments

I/R injury and MI were performed in 12±2-week-old mice as described[9,10] (online supplement). Control mice underwent a thoracotomy only (sham).

Transthoracic Echocardiography and Hemodynamics

Left ventricle (LV) hemodynamics were measured as described.[10] The right jugular vein was cannulated for infusion of dobutamine (4 μg/kg per min up to 40 μg/kg per min; online supplement). Echocardiography was performed in sedated mice (ketamine, 100 mg/kg IP and xylazine, 1.25 mg/kg IP) as described[11] (online supplement).

Langendorff Preparations

Langendorff preparations were performed as described.[12]

Metabolic Assay

Measurement of heart tissue levels of lactate, ATP, ADP, and AMP with high-performance liquid chromatography were described[13,14] (online supplement).

Quantification of I/R and MI Injury

After I/R, area at risk and early infarct size were assessed by Evan's blue and 2,3,5-triphenyltetrazolium chloride staining.[10] After I/R (7 days), respectively after permanent coronary ligation, MI sizes were determined in myocardial sections fixed in situ and stained with hematoxylin/eosin (H&E).[10]

Treatment of Mice With an Agonistic Anti-Fas Antibody

Monoclonal anti-mouse Fas IgG (10 μg Jo2; Pharmingen) or antitrinitrophenol control IgG (Pharmingen) was injected intraperitoneally. After 24 hours, cryosections were prepared from the LV.[15]

Histological Analyses, Immunostaining, and Electron Microscopy

LV tissue slices were stained with Sirius red F3BA, van Gieson, or H&E, as described.[10] Interstitial collagen volume fraction was determined in picro-Sirius red F3BA-stained sections (online supplement).[10] Apoptotic nuclei were detected by TUNEL, and apoptotic morphology of nuclei was confirmed by counterstaining with Hoechst 33258 (Sigma; online supplement).[15] Immunohistochemistry was performed with antibodies recognizing the C terminus of the STAT3 protein (Cell Signaling Technology), sarcomeric α-actinin (Sigma), platelet-endothelial cell adhesion molecule-1 (PECAM-1), tissue inhibitor of metalloproteinase-1 (TIMP1), or thrombospondin-1 (TSP1; Santa Cruz Biotechnology). Additional LV tissue samples were analyzed by electron microscopy.[16]

LV capillary density was determined either as the ratio of PECAM-1–positive cells to total nuclei (hematoxylin or Hoechst stain) or as capillary to cardiomyocytes ratio in van Gieson or PECAM-1/wheat germ agglutinin (WGA; Vector Laboratories)–stained LV sections (online supplement). Density of coronary resistance vessels (Ø 25 to 150 μm) was determined on H&E-stained LV sections (online supplement).

DNA Laddering

Genomic DNA was isolated from LV tissue and separated on a 1.4% agarose gel (35 μg per lane).

RT-PCR, Northern, and Immunoblot Analyses

Northern blotting and RT-PCR were performed according to standard procedures[17] using primers, cDNA, and oligonucleotide probes described in the online supplement. Antibodies against vascular endothelial growth factor (VEGF), hypoxia-inducible factor-1α (HIF1α), basic fibroblast growth factor (bFGF), TIMP1, TSP1 (Santa Cruz Biotechnology), IL-15 (R&D), STAT3, and tyrosine phosphorylation (phospho-Tyr)–STAT3 (Cell Signaling Technology) were used for immunoblots.

Cell Culture

Cardiomyocytes from 3- to 4-month-old wild-type (WT) and knockout (KO) mice were isolated using 0.04% collagenase (Worthington) and plated in DMEM/medium 199 (M199)/5% FCS/10% horse serum on culture dishes for 24 hours, and then the medium was changed to serum-free DMEM/M199 for an additional 12 hours. Cell proliferation was assessed in mouse embryonic fibroblasts (MEFs) and in primary cultures of adult mouse lung endothelial cells (MLECs) by determining [^{3}H]-thymidine incorporation (online supplement).

cDNA Expression Microarray Analysis

Total LV RNA was isolated from 3- to 4-month-old WT and KO mice, reverse transcribed into Cy3-dCTP– and Cy5-dCTP–labeled cDNA probes, and hybridized to Parallel Identification and Quantification of RNA Immuno/Onco cDNA microarrays, containing cDNA sequences from 648 mouse genes (Biozym Diagnostik). To minimize intragroup variation, cDNA probes from 5 hearts per genotype were pooled.

Statistical Analyses

Data are presented as mean±SD. Differences between groups were analyzed by Mann–Whitney test, Student *t* test, or log-rank test, as appropriate. A 2-tailed $P<0.05$ was considered statistically significant.

Results

Cardiomyocyte-Restricted STAT3 Deletion

Mice with a cardiomyocyte-restricted STAT3 deletion were generated by mating *STAT3*$^{flox/flox}$ with transgenic mice expressing Cre-recombinase under control of the αMHC promoter (*αMHC-Cre*$^{tg/-}$), which directs transgene expression to cardiomyocytes (Figure 1). The efficiency and specificity of αMHC-Cre–mediated deletion of floxed genes have been demonstrated previously.[8,18] *αMHC-Cre*$^{tg/-}$; *STAT3*$^{flox/flox}$ (KO), *STAT3*$^{flox/flox}$ (WT), and heterozygous mice (*αMHC-Cre*$^{tg/-}$; *STAT3*$^{flox/+}$) were born according to Mendelian inheritance ratios, survived into adulthood, and were fertile. PCR analyses of genomic DNA confirmed complete Cre/loxP recombination in cardiomyocytes isolated from 3-month-old KO mice (Figure 1A). Shortly after birth, STAT3 protein levels were reduced by ≈40% in isolated cardiomyocytes from KO compared with WT mice; LV STAT3 protein levels then gradually decreased in KO mice, resulting in a virtually complete, cardiomyocyte-restricted STAT3 deletion at the age of 3 months (Figure 1B). The faint band of STAT3 protein observed in LV extracts from KO mice represents expression in noncardiomyocytes, as shown by immunohistochemistry (Figure 1C through 1E). Heterozygotes, expressed slightly lower amounts of STAT3 protein compared with WT mice but were not significantly different from WT in terms of survival and cardiac performance in all experiments (data not shown).

Reduced Myocardial Capillarization and Enhanced Fibrosis in STAT3 KO Mice

LV to body weight ratios and cardiac dimensions (Table), cardiomyocyte ultrastructure (Figure 2A), and expression

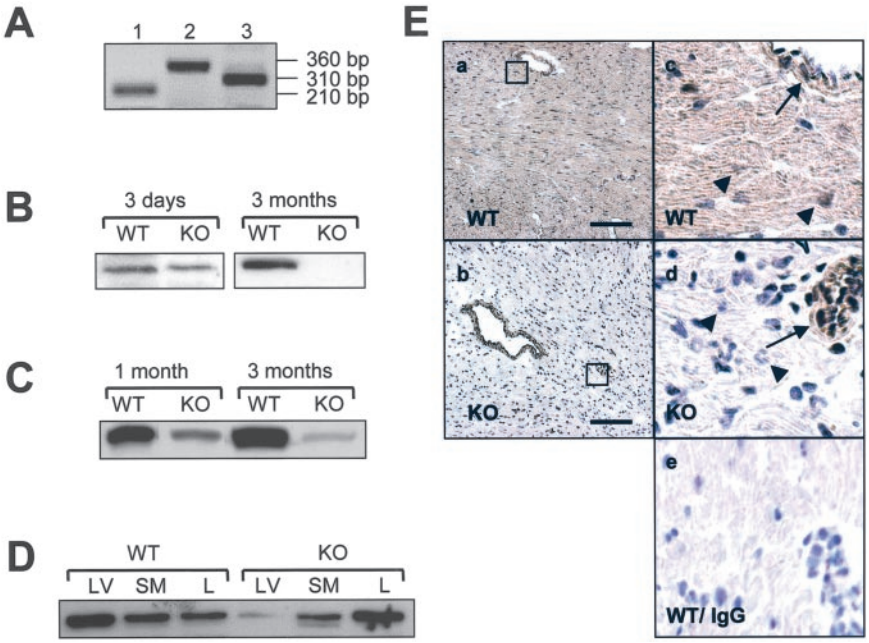

Figure 1. Cardiomyocyte-specific STAT3 deletion. A, Genomic PCR analysis of isolated cardiomyocytes from 3-month-old *STAT3*$^{+/+}$ (lane 1), *STAT3*$^{flox/flox}$ (lane 2), and KO (lane 3) mice. B, STAT3 protein expression in isolated cardiomyocytes from neonatal and 3-month-old WT and KO mice. C, STAT3 protein expression in LVs from 1- and 3-month-old WT and KO mice. D, STAT3 protein expression in LV, skeletal muscle (SM), and liver (L) from WT and KO mice (3 months). E, Cell-specific expression of STAT3 protein (brown staining) in representative LV sections (counterstained with hematoxylin, purple nuclei) of 3-month-old WT (a and c) and KO mice (b and d). c and d show higher magnification (×400) of the framed area in a and b, respectively. Arrows point to nuclei of cells in the vascular wall; arrowheads point to cardiomyocytes nuclei. Control slide (e) was stained with nonspecific IgG. (Bars=100 μm).

levels of αMHC, βMHC, skeletal muscle (SkM) α-actin, sarco(endo)plasmic reticulum Ca^{2+}-ATPase-2a (SERCA2a), and atrial natriuretic peptide (ANP) mRNA (Figure 2B) did not differ in 3- to 4-month-old WT and KO mice. However, STAT3 deletion in cardiomyocytes resulted in reduced LV capillarization, as shown by anti–PECAM-1/WGA immunohistochemistry (Figure 2C), and confirmed in van Gieson–stained sections (capillary to cardiomyocyte ratio 1.6±0.2 versus 1.0±0.2 in WT and KO; n=6 each; $P<0.01$). Reduced myocardial capillary density in KO mice was slowly evolving after birth and was significant at the age of 8 to 12 weeks (Figure 2D), indicating that STAT3 in cardiomyocytes is required postnatally for myocardial capillary growth. Average density of coronary resistance vessels (Ø 25 to 150 μm) was similar in WT and KO mice (online supplement). Basal and peak coronary flow, known to be regulated primarily by coronary resistance vessels rather than capillaries,[19] were not altered in Langendorff-perfused KO hearts (data not shown). However, KO hearts displayed lower heart rates (KO 506±17 versus WT 565±17 bpm; $P<0.01$) and lower dP/dt(max) (KO 6662±1075 versus WT 8033±509 mm Hg per sec; $P=0.08$) after administration of dobutamine, a β-adrenergic agonist (n=6 each; online supplement). The lactate concentration was significantly increased (KO 5.6±0.7 versus WT 3.4±1.3 μmol/g; $P<0.02$) and the ratio of high-energy phosphate ATP to ADP tended to be lower (KO 0.75±0.15 versus WT 0.98±0.22, $P=0.06$) in KO versus WT LVs after dobutamine infusion (KO n=4; WT n=5; online supplement). Interstitial collagen volume fraction was increased moderately in 3- to 4-month-old KO mice (Figure 2E; WT 0.15±0.08% versus KO 0.33±0.10%; n=5 each; $P<0.05$) and strongly augmented in 6-month-old KO mice (0.18±0.05% versus 0.82±0.20% in WT and KO; n=4 each; $P<0.01$).

Reduced capillary density and enhanced interstitial fibrosis in KO suggested that STAT3 controls expression of downstream genes in cardiomyocytes that may be involved in regulation of myocardial capillarization or fibrosis. However, protein expression levels of HIF-1α, VEGF, and bFGF (genes known to be critically involved in angiogenesis) were not

Cardiac Morphology and Function in WT and STAT3 KO Mice

	WT Basal	KO Basal	WT I/R (7 days)	KO I/R (7 days)	WT MI (14 days)	KO MI (14 days)
LVEDD (mm)	4.1±0.2	4.0±0.2	4.0±0.4	4.2±0.2	5.1±0.4**§§	5.5±0.3**§§
LVESD (mm)	2.7±0.3	2.6±0.1	2.8±0.5	3.2±0.5*§†	4.1±0.6**§§	4.6±1.0**§§
FS (%)	35±5	33±4	32±3	22±3**§§†	20±7**§§	12±4**§§##
HR (bpm)	298±74	277±48	254±45	233±468	351±32	320±31
LV/BW (mg/g)	3.0±0.2	3.1±0.4	3.2±0.4	3.1±0.4	4.9±0.5**§§	4.8±0.9**§§
CSA (μm^2)	259±28	231±9			505±115**§§	361±38*§§#

LV end-diastolic diameter (LVEDD), LV end-systolic diameter (LVESD), fractional shortening (FS) and heart rate (HR) were determined by echocardiography. Cardiomyocyte cross-sectional area (CSA) was determined in in situ–fixed LV sections.

*$P<0.05$; **$P<0.01$ vs basal WT; §$P<0.05$; §§$P<0.01$ vs basal KO; †$P<0.05$; ††$P<0.01$ WT vs KO after I/R; #$P<0.05$; ##$P<0.01$ WT vs KO after MI; n=5 to 8 animals per group.

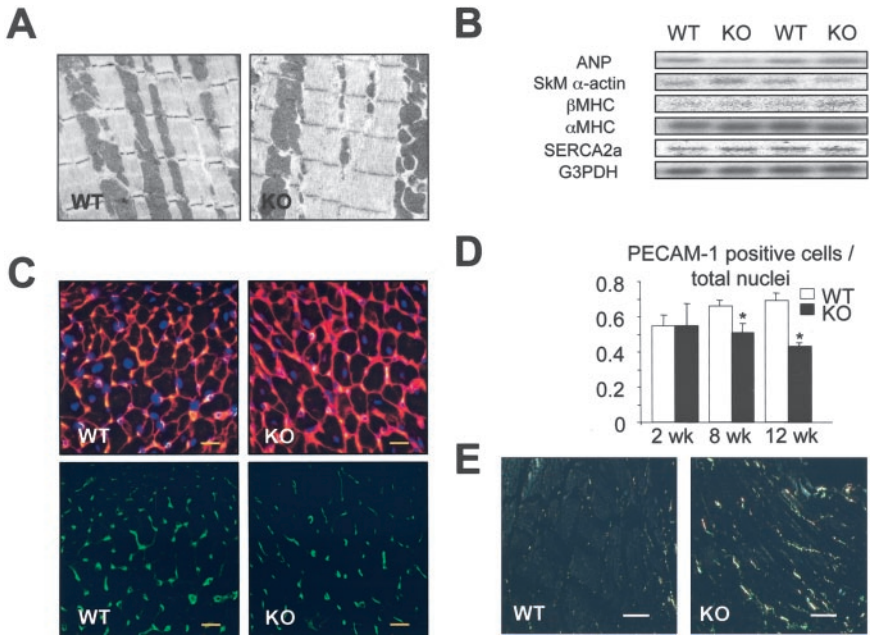

Figure 2. Cardiac phenotype of 3-to 4-month-old KO mice. A, No abnormalities in sarcomere or mitochondrial ultrastructure are found by electron microscopy in KO LVs. B, Expression of ANP, αMHC, βMHC, SkM α-actin, SERCA2a, and G3PDH transcripts. C, Capillaries in WT and KO LV sections are identified by anti–PECAM-1 immunohistochemistry (green); WGA stain marks cell membranes (red); and Hoechst stain identifies nuclei (blue). D, Bar graph summarizing ratio of PECAM-1–positive cells/total nuclei in WT and KO LV sections at 2, 8, and 12 weeks of age (n=4 per genotype and time point; *$P<0.05$ vs corresponding WT). E, Slightly enhanced deposition of interstitial collagen in KO LVs (picro-Sirius red stain; bars in C=25 μm; bars in E=50 μm).

different in LVs from KO and WT (Figure 3A). To identify additional candidate genes, cDNA probes derived from LVs of 3- to 4-month-old WT and KO were hybridized to custom-made cDNA microarrays containing 648 genes, including genes putatively involved in angiogenesis or control of interstitial matrix composition (online supplement). Genes differing in their expression levels >1.8-fold were considered differently expressed (Figure 3B). For some of these genes, differential expression was confirmed independently by RT-PCR, Northern blotting, immunoblotting, or immunohistochemistry in at least n=4 mice of each genotype (Figure 3A through 3D; data not shown). Overall, the cDNA microarray analyses revealed a shift in gene expression pattern consistent with a profibrotic and antiangiogenic state, with increased expression levels of collagen-1α (COL1A1), COL8A1, osteopontin (OPN), biglycan, tenascin-C (TNC), plasminogen activator inhibitor-1 (PAI-1), connective tissue growth factor (CTGF), TSP1, and TIMP1[20–24] (Figure 3B), whereas expression of matrix metalloproteinase type 2 (MMP-2) and MMP-9 was unchanged (data not shown). Several of these factors, including CTGF, TSP1, and TIMP1, are known to be potent antiangiogenic factors.[25–27] For example, CTGF and TSP1 have been shown previously to inhibit VEGF angiogenic activity.[25,26] Immunohistochemistry demonstrated enhanced TIMP1 and TSP1 levels associated with the extracellular matrix in KO (Figure 3C and 3D). Furthermore, isolated cardiomyocytes from KO mice displayed increased protein abundance of TIMP1 and TSP1 (data not shown). Because the antiangiogenic activity of TSP1 depends, in part, on Fas-mediated endothelial cell apoptosis,[28] we injected an agonistic anti-Fas antibody into KO and WT mice (n=5 each). As determined by TUNEL/Hoechst-staining and anti–PECAM-1 immunohistochemistry, stimulation of the Fas receptor promoted significantly more endothelial cell apoptosis in KO LVs (0.033‰ versus 0.013‰; $P<0.05$).

The presence of paracrine factors released by KO cardiomyocytes was confirmed by the finding that KO cardiomyocytes supernatant induced a higher proliferation rate in fibroblasts (MEFs) and a lower proliferation rate in endothelial cells (MLECs) compared with WT cardiomyocytes supernatant (Figure 3E).

Cardiomyopathy With Massive Fibrosis and High Mortality During Long-Term Follow-Up in STAT3 KO Mice

Beyond 9 months, KO mice displayed an enhanced mortality rate (Figure 4A). Decreased survival in KO mice was associated with heart failure symptoms such as labored breathing and generalized edema (data not shown). At 12 months, the hearts of KO mice were dilated (Figure 4B and 4F) with massive interstitial fibrosis (Figure 4C) and increased rate of apoptosis (mainly nonmyocytes because most TUNEL-positive nuclei were located in cells negative for sarcomeric α-actinin; data not shown; Figure 4D), along with substantially enhanced expression levels of ANP (+297%; $P<0.01$), SkM α-actin (+85%; $P<0.05$), TIMP1 (+900%; $P<0.01$), TSP1 (+317%; $P<0.01$), and the proapoptotic Bcl-2 family member Bcl-2/adenovirus EIB 19kD-interacting protein 3 (BNIP3;[29] +78%; $P<0.05$), whereas βMHC and SERCA2a expression were not significantly altered compared with WT (Figure 4E). Furthermore, KO mice showed impaired cardiac contractile function (Figure 4F). Heart rate was similar in both genotypes (data not shown).

Increased Susceptibility to I/R Injury in STAT3 KO Mice

In WT mice, ischemia for 1 hour, followed by reperfusion for 1 hour or 24 hours, induced rapid phospho-Tyr of STAT3 in the remote (nonischemic) and reperfused (I/R) LV. In contrast, only faint STAT3-phosphorylation was observed in KO mice, presumably because of STAT3 activation in noncardiomyocytes (Figure 5A). The area at risk during left anterior descending (LAD) occlusion was similar in WT and KO mice (Figure 5B). However, infarct sizes after 24 hours of reper-

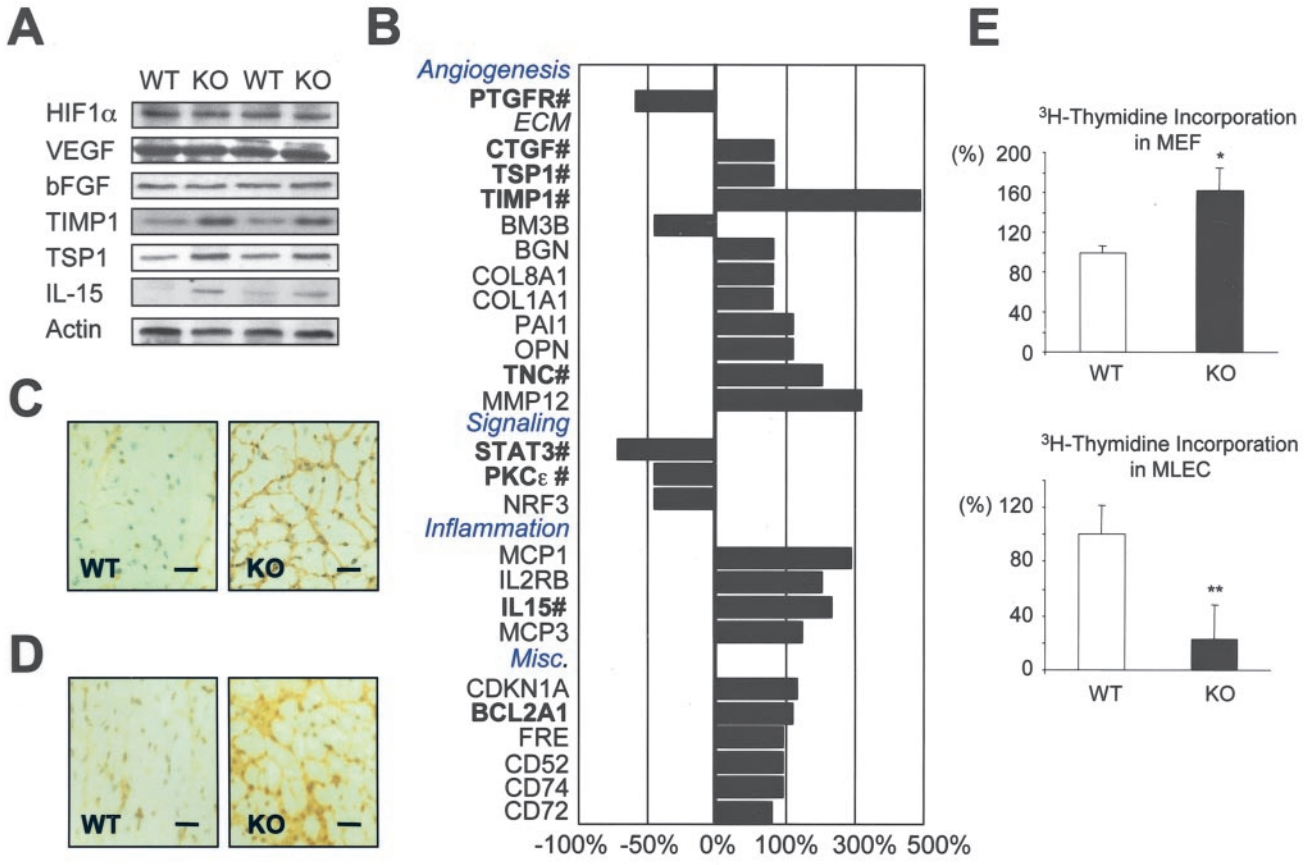

Figure 3. A, Representative immunoblots showing HIF1α, VEGF, bFGF, TIMP1, TSP1, IL-15, and actin expression in WT and KO LVs. B, cDNA microarray analysis: genes differing in their expression levels >1.8-fold are shown (positive values upregulated in KO). Expression levels of genes highlighted in bold were evaluated in independent experiments by RT-PCR, Northern blotting, or immunoblotting (#differential expression confirmed). Immunohistochemistry shows elevated TIMP1 (C) and TSP1 (D) protein abundance in the extracellular matrix in KO LVs (bars in B, C, E, H, J=25 μm). E, Bar graph showing [3H]-thymidine incorporation in MEFs or MLECs after exposure to supernatant of isolated WT or KO cardiomyocytes (n=4 individual preparations per genotype; *$P<0.05$; **$P<0.01$).

fusion were significantly greater in KO LVs (Figure 5B), and this was associated with enhanced apoptosis in cardiomyocytes in the reperfused area (Figure 5C and 5D; immunohistochemistry for caspase-3 in online supplement). No increases in apoptotic nuclei were observed in the remote myocardium after I/R (24 hours) in either genotype (data not shown). After I/R (24 hours), both genotypes displayed similar increases in transcript levels of VEGF (452±240% versus 451±102% in WT and KO), Bcl-2 (349±130% versus 447±128% in WT and KO), and Bcl-X (354±92% versus 396±160% in WT and KO). In contrast, BNIP3 induction in KO was more pronounced (2.2±0.9-fold versus WT; $P<0.05$; Figure 5D), whereas induction of cardioprotective heat shock protein 70 (HSP70)[30] was lower (KO 333±86% versus WT 648±13%; $P<0.05$; Figure 5D). Moreover, fractional shortening after I/R (7 days) was significantly impaired in KO mice (Table).

Reduced Cardiac Function and Increased Mortality After MI in STAT3 KO Mice

Permanent LAD ligation caused a striking increase in mortality in KO mice; After 6 months, 21 of 21 KO mice (100%) but only 6 of 19 WT mice (32%) had died (Kaplan–Meier curve; online supplement). All sham-operated KO and WT mice (n=6 each) survived 6 months. Two weeks after MI, KO mice showed larger infarct sizes (WT, n=6 37±9% versus KO, n=7 51±12%; $P<0.05$), a more pronounced deterioration in LV systolic function (Table), an attenuated increase in cardiomyocyte cross-sectional area (Table), and more interstitial fibrosis in the remote LV (KO 0.80±0.24% versus WT 0.36±0.16%; $P<0.05$).

Discussion

Postnatal heart growth is accompanied by a proportional growth of the capillary network and interstitial matrix.[31] Paracrine factors from cardiomyocytes have been postulated to play a pivotal role in this process;[32] however, the molecular mechanisms of this intercellular cross-talk are poorly understood. Here, we present evidence that STAT3 in cardiomyocytes controls paracrine circuits essential for postnatal maintenance of capillary vasculature and balance of interstitial matrix deposition.

Previous studies have indicated that overexpression or activation of STAT3 in cardiomyocytes enhances VEGF expression, which, in turn, promotes myocardial capillary formation,[33] whereas cardiomyocyte-specific deletion of

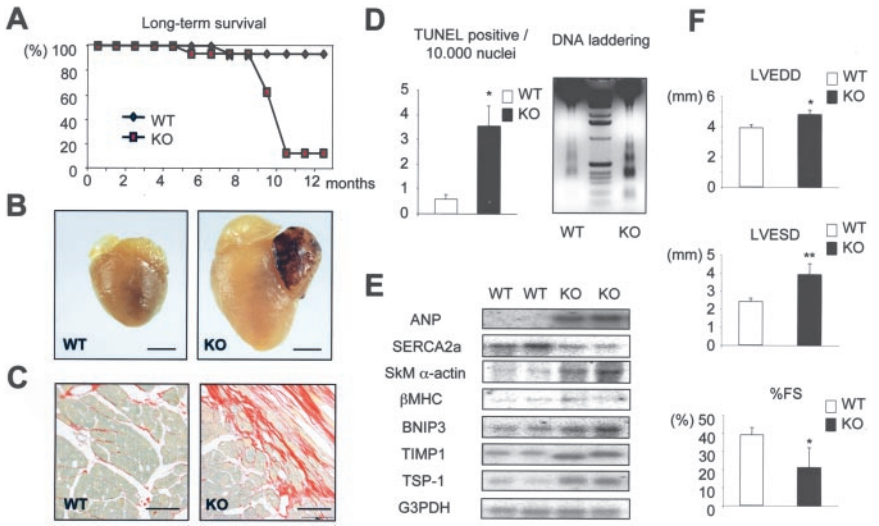

Figure 4. Heart failure in KO mice within 1 year of follow-up. A, Kaplan–Meier curves depicting long-term survival of WT (n=16) and KO mice (n=16; $P<0.001$ by log-rank test). B, Four-chamber dilatation (and a left atrial thrombus) in a 1-year-old KO heart; for comparison, an age-matched WT heart is shown (bars=2.5 mm). C, Sirius red staining shows extensive LV fibrosis (red) in a representative 1-year-old KO LV (bars=100 μm). D, LV apoptosis as detected by TUNEL/Hoechst staining and DNA laddering. E, Expression of ANP, SkM α-actin, βMHC, SERCA2a, BNIP3, TIMP1, TSP1, and G3PDH in LVs from 1-year-old KO and WT mice. F, Left ventricular end-diastolic dimension (LVEDD), left ventricular end-systolic diameter (LVESD), and percentage of fractional shortening (%FS) as determined by echocardiography (n=4 to 6 per genotype; *$P<0.05$; **$P<0.05$ vs WT).

VEGF reduces coronary microvascularization,[34] suggesting that VEGF may be an important target gene mediating proangiogenic effects of STAT3. However, VEGF expression was not reduced in KO hearts, indicating that STAT3-dependent postnatal capillary growth does not involve VEGF expression regulation. Moreover, I/R-induced VEGF upregulation was similar in WT and KO mice, indicating that STAT3 in cardiomyocytes is not required for VEGF upregulation after I/R injury. Remarkably, KO mice displayed an upregulation of CTGF, an endogenous inhibitor of VEGF activity,[26] and increased expression levels of TSP1, which suppresses capillary formation by inhibiting VEGF release and inducing endothelial cell apoptosis.[25,28,35] Moreover, expression of the potent antiangiogenic factor TIMP1[27] was augmented in KO hearts.

Several antiangiogenic factors are also involved in the formation of interstitial matrix (eg, CTGF, TSP1, TIMP1, OPN, TNC, and PAI-1).[20–24] All of these genes are upregulated in KO mice, which is consistent with the profibrotic state in these animals. Vice versa, there is evidence that enhanced interstitial matrix formation inhibits angiogenesis,[36] supporting the concept that the antiangiogenic and profibrotic cardiac phenotypes of KO mice are mediated, at least in part, by overlapping paracrine mechanisms. A potential cardiomyocyte-dependent paracrine mechanism promoting fibrosis and inhibiting angiogenesis in KO mice is supported by the observation that supernatant of cultured KO cardiomyocytes inhibited proliferation in endothelial cells and enhanced fibroblast proliferation. Although the cell type(s) expressing antiangiogenic or profibrotic factors and the precise molecular pathways controlling capillarization and interstitial matrix composition in KO mice have not been addressed in this study, our in vitro data suggest that STAT3 controls release of paracrine factors by cardiomyocytes that directly affect the phenotype of endothelial cells and fibroblasts. In addition, our microarray analyses have uncovered several candidate mechanisms whereby STAT3 ablation in cardiomyocytes inhibits capillary formation and promotes interstitial fibrosis in the myocardium. It is considerable that the STAT3 impact on angiogenesis and interstitial matrix is not related to altered expression of a single gene, but rather to differential expression of an array of genes involved in the fine tuning of interstitial matrix deposition and angiogenesis.

There could be alternative explanations for the enhanced fibrosis in KO myocardium, such as replacement fibrosis caused by myocyte loss as a result of decreased myocardial blood supply or oxidative stress secondary to tissue hypoxia/ischemia driving fibrosis. Although we did not observe enhanced apoptosis or upregulation of hypoxia markers such as HIF1α or BNIP3 in young KO mice under normal conditions, impaired cardiac perfusion and metabolism became obvious during dobutamine stress and resulted in increased lactate production. In addition, a recent report by Jacoby et al[37] suggested that the STAT3 pathway is required to suppress inflammation, and thus reactive fibrosis may arise in response to low levels of inflammation. In this context, there is evidence that STAT3 can act as a direct transcriptional inhibitor for nuclear factor κB–mediated gene expression.[38]

Previous studies using cell-specific overexpression of STAT3 have identified several target genes for STAT3, including VEGF and the Bcl-2 family of antiapoptotic proteins.[39] However, endogenous STAT3 does not appear to be required for expression of VEGF and Bcl-2 family members (Bcl-2, Bcl-X) in the heart. In this regard, it should be noted that the expression levels of the proapoptotic Bcl-2 family member BNIP3 were not altered in young KO mice but were significantly increased only in aged KO mice (presenting with heart failure) or in KO mice after I/R injury. Thus, it appears that the upregulation of BNIP3 is secondary, possibly related to myocardial hypoxia, resulting from reduced capillary density and increased interstitial fibrosis.[29]

Development of severe cardiac fibrosis in aging KO mice was associated with impaired cardiac function, increased apoptosis, ventricular remodeling, and heart failure with generalized edema and enhanced mortality (ie, typical features noted in patients with dilated cardiomyop-

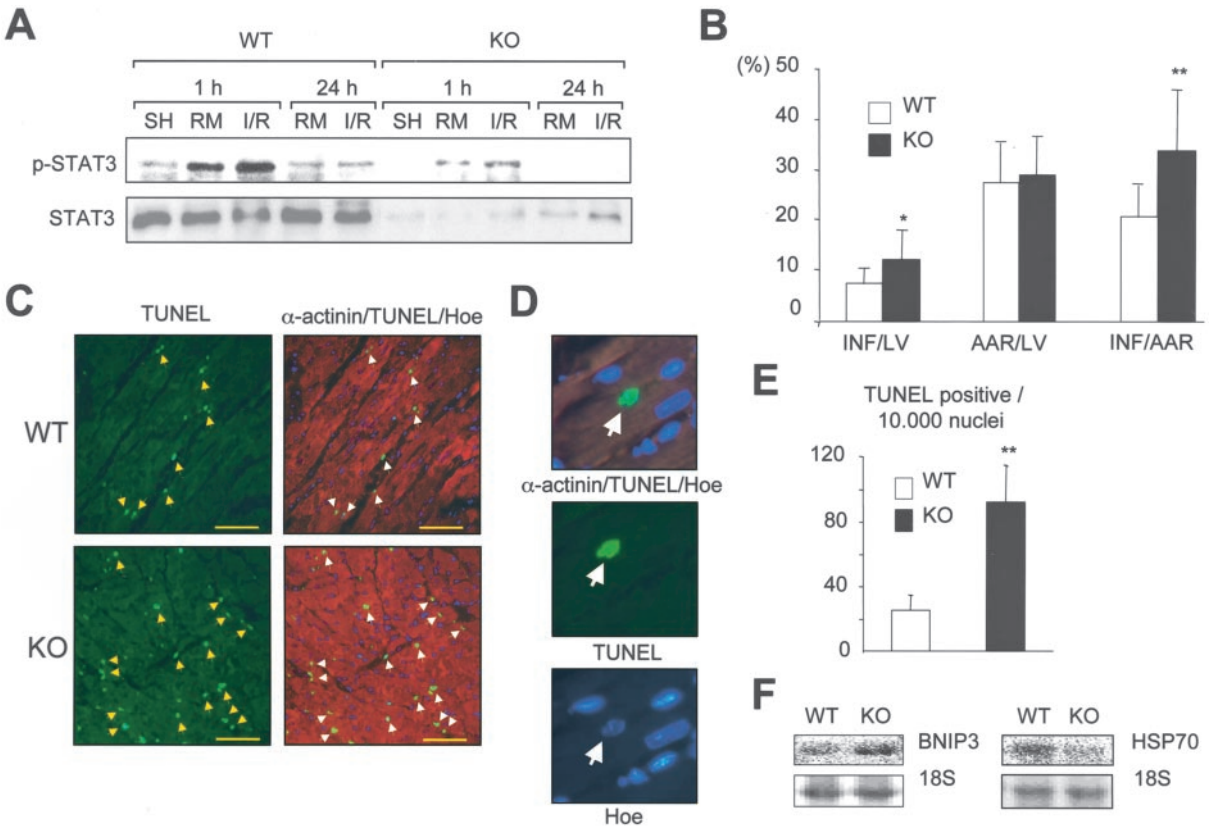

Figure 5. Increased susceptibility to I/R injury in KO mice (3 months of age). A, Immunoblots showing phospho-Tyr–STAT3 and STAT3 in WT and KO LVs after ischemia (1 hour) and reperfusion for 1 hour or 24 hours (SH indicates LV from sham-operated mice; RM, remote LV; I/R, reperfused LV). B, Bar graph showing infarcted area (INF) and area at risk (AAR) expressed as percentage of total LV and INF calculated as percentage of AAR in WT (n=9) and KO (n=10) mice subjected to I/R (24 hours; *$P<0.05$; **$P<0.01$ vs WT). C, TUNEL staining (green, arrows, left panels) shows more apoptotic nuclei in LV areas exposed to ischemia (1 hour) and reperfusion (24 hours) in KO compared with WT mice. Right panels show the same sections with triple staining: green, TUNEL-positive apoptotic nuclei (arrows); blue, Hoechst stain (Hoe, marks nuclear chromatin) labeling TUNEL-negative nuclei; red, sarcomeric α-actinin (α-actinin) marking cardiomyocytes. Bars=50 μm. D, Top, Triple staining identifies an apoptotic cardiomyocyte nucleus (green–blue, arrow), double stained for TUNEL and Hoe, surrounded by normal nuclei (blue); red, α-actinin. Middle panel shows same area with TUNEL stain only (apoptotic cardiomyocyte nucleus, green, arrow). Bottom shows same area with Hoechst stain only, indicating fragmented nuclear chromatin of the apoptotic cardiomyocyte nucleus (arrow). E, Bar graph summarizes apoptotic nuclei in the border zone (n=6 of each genotype; **$P<0.01$ vs WT) associated with (F) augmented expression of BNIP3, respectively attenuated expression of HSP70 (representative Northern blots).

athy and end-stage heart failure). We have shown previously that STAT3 protein abundance and activation are markedly reduced in failing human hearts.[6] Therefore, it is conceivable that reduced STAT3 expression and activation in patients with heart failure adversely affect fundamental cardioprotective mechanisms (in analogy to what is observed in our KO mice), thereby contributing to the progression of heart failure.

As revealed by morphometric, molecular, and functional analyses of KO mice, STAT3 is critically involved in myocardium response to I/R. Infarct sizes after I/R injury were increased in KO hearts, and this was associated with a significant increase in myocardial apoptosis. Previous studies have shown that STAT3 exerts direct cytoprotective effects in cardiomyocytes subjected to ischemia or toxic stress.[5,40] The attenuated HSP70 induction in KO myocardium after I/R, a gene known to be transcriptionally regulated by STAT3[41] and to be involved in protection of the heart from I/R injury,[30] suggests that STAT3 exerts at least some of its cardioprotective effects via induction of HSPs. In addition, impaired myocardial capillarization in KO mice may contribute to larger infarcts and enhanced cardiomyocytes apoptosis (eg, by impeding tissue oxygenation during reperfusion). In support of such a concept, induction of BNIP3, which has been identified recently as a hypoxia-regulated inducer of cardiomyocyte death,[29] was more pronounced in KO compared with WT mice after I/R injury. In addition, impaired metabolic capacity resulting from reduced perfusion and lower tissue oxygenation during sympathetic stress, as simulated by dobutamine infusion, together with larger infarct size, more interstitial fibrosis, and attenuated hypertrophy, may contribute to the impaired cardiac function and heart failure observed in KO mice after MI. Thus, these data support the concept that STAT3 in cardiomyocytes is providing cardioprotection and cardiac adaptation to I/R and ischemic injury.

In conclusion, STAT3 in cardiomyocytes plays a critical role in myocardium adaptation to stress by maintaining

myocardial capillarization, controlling interstitial collagen metabolism, protecting from apoptosis, and preserving cardiac function. STAT3 activation (eg, by IL-6 family members) may therefore represent a beneficial mechanism that should be maintained rather than blocked in patients with heart failure.

Acknowledgments

This study was supported by the Deutsche Forschungsgemeinschaft, the Jean Leducq Foundation, and the Italian Ministry of University and Research. We are indebted to Silvia Gutzke, Birgit Brandt, and Dr Peter Lippolt for expert technical assistance.

References

1. Negoro S, Kunisada K, Tone E, Funamoto M, Oh H, Kishimoto T, Yamauchi-Takihara K. Activation of JAK/STAT pathway transduces cytoprotective signal in rat acute myocardial infarction. *Cardiovasc Res*. 2000;47:797–805.
2. Xuan YT, Guo Y, Han H, Zhu Y, Bolli R. An essential role of the JAK-STAT pathway in ischemic preconditioning. *Proc Natl Acad Sci U S A*. 2001;98:9050–9055.
3. Yasukawa H, Hoshijima M, Gu Y, Nakamura T, Pradervand S, Hanada T, Hanakawa Y, Yoshimura A, Ross J Jr, Chien KR. Suppressor of cytokine signaling-3 is a biomechanical stress-inducible gene that suppresses gp130-mediated cardiac myocyte hypertrophy and survival pathways. *J Clin Invest*. 2001;108:1459–1467.
4. Funamoto M, Fujio Y, Kunisada K, Negoro S, Tone E, Osugi T, Hirota H, Izumi M, Yoshizaki K, Walsh K, Kishimoto T, Yamauchi-Takihara K. Signal transducer and activator of transcription 3 is required for glycoprotein 130-mediated induction of vascular endothelial growth factor in cardiac myocytes. *J Biol Chem*. 2000;275:10561–10566.
5. Negoro S, Kunisada K, Fujio Y, Funamoto M, Darville MI, Eizirik DL, Osugi T, Izumi M, Oshima Y, Nakaoka Y, Hirota H, Kishimoto T, Yamauchi-Takihara K. Activation of signal transducer and activator of transcription 3 protects cardiomyocytes from hypoxia/reoxygenation-induced oxidative stress through the upregulation of manganese superoxide dismutase. *Circulation*. 2001;104:979–981.
6. Podewski EK, Hilfiker-Kleiner D, Hilfiker A, Morawietz H, Lichtenberg A, Wollert KC, Drexler H. Alterations in Janus kinase (JAK)-signal transducers and activators of transcription (STAT) signaling in patients with end-stage dilated cardiomyopathy. *Circulation*. 2003;107:798–802.
7. Alonzi T, Maritano D, Gorgoni B, Rizzuto G, Libert C, Poli V. Essential role of STAT3 in the control of the acute-phase response as revealed by inducible gene inactivation [correction of activation] in the liver. *Mol Cell Biol*. 2001;21:1621–1632.
8. Gaussin V, Van de Putte T, Mishina Y, Hanks MC, Zwijsen A, Huylebroeck D, Behringer RR, Schneider MD. Endocardial cushion and myocardial defects after cardiac myocyte-specific conditional deletion of the bone morphogenetic protein receptor ALK3. *Proc Natl Acad Sci U S A*. 2002;99:2878–2883.
9. Dumont EA, Hofstra L, van Heerde WL, van den Eijnde S, Doevendans PA, DeMuinck E, Daemen MA, Smits JF, Frederik P, Wellens HJ, Daemen MJ, Reutelingsperger CP. Cardiomyocyte death induced by myocardial ischemia and reperfusion: measurement with recombinant human annexin-V in a mouse model. *Circulation*. 2000;102:1564–1568.
10. Fuchs M, Hilfiker A, Kaminski K, Hilfiker-Kleiner D, Guener Z, Klein G, Podewski E, Schieffer B, Rose-John S, Drexler H. Role of interleukin-6 for left ventricular remodeling and survival after experimental myocardial infarction. *FASEB J*. 2003;17:2118–2120.
11. Schaefer A, Klein G, Brand B, Lippolt P, Drexler H, Meyer GP. Evaluation of left ventricular diastolic function by pulsed Doppler tissue imaging in mice. *J Am Soc Echocardiogr*. 2003;16:1144–1149.
12. Godecke A, Flogel U, Zanger K, Ding Z, Hirchenhain J, Decking UK, Schrader J. Disruption of myoglobin in mice induces multiple compensatory mechanisms. *Proc Natl Acad Sci U S A*. 1999;96:10495–10500.
13. Martin C, Schulz R, Rose J, Heusch G. Inorganic phosphate content and free energy change of ATP hydrolysis in regional short-term hibernating myocardium. *Cardiovasc Res*. 1998;39:318–326.
14. Martin C, Schulz R, Post H, Gres P, Heusch G. Effect of NO synthase inhibition on myocardial metabolism during moderate ischemia. *Am J Physiol Heart Circ Physiol*. 2003;284:H2320–H2324.
15. Wollert KC, Heineke J, Westermann J, Ludde M, Fiedler B, Zierhut W, Laurent D, Bauer MK, Schulze-Osthoff K, Drexler H. The cardiac Fas (APO-1/CD95) receptor/Fas ligand system: relation to diastolic wall stress in volume-overload hypertrophy in vivo and activation of the transcription factor AP-1 in cardiac myocytes. *Circulation*. 2000;101:1172–1178.
16. Schmiedl A, Schnabel PA, Mall G, Gebhard MM, Hunneman DH, Richter J, Bretschneider HJ. The surface to volume ratio of mitochondria, a suitable parameter for evaluating mitochondrial swelling. Correlations during the course of myocardial global ischaemia. *Virchows Arch A Pathol Anat Histopathol*. 1990;416:305–315.
17. Wollert KC, Taga T, Saito M, Narazaki M, Kishimoto T, Glembotski CC, Vernallis AB, Heath JK, Pennica D, Wood WI, Chien KR. Cardiotrophin-1 activates a distinct form of cardiac muscle cell hypertrophy. Assembly of sarcomeric units in series VIA gp130/leukemia inhibitory factor receptor-dependent pathways. *J Biol Chem*. 1996;271:9535–9545.
18. Holtwick R, van Eickels M, Skryabin BV, Baba HA, Bubikat A, Begrow F, Schneider MD, Garbers DL, Kuhn M. Pressure-independent cardiac hypertrophy in mice with cardiomyocyte-restricted inactivation of the atrial natriuretic peptide receptor guanylyl cyclase-A. *J Clin Invest*. 2003;111:1399–1407.
19. Marcus ML, Chilian WM, Kanatsuka H, Dellsperger KC, Eastham CL, Lamping KG. Understanding the coronary circulation through studies at the microvascular level. *Circulation*. 1990;82:1–7.
20. Chua CC, Hamdy RC, Chua BH. Regulation of thrombospondin-1 production by angiotensin II in rat heart endothelial cells. *Biochim Biophys Acta*. 1997;1357:209–214.
21. Imanaka-Yoshida K, Hiroe M, Nishikawa T, Ishiyama S, Shimojo T, Ohta Y, Sakakura T, Yoshida T. Tenascin-C modulates adhesion of cardiomyocytes to extracellular matrix during tissue remodeling after myocardial infarction. *Lab Invest*. 2001;81:1015–1024.
22. Katoh M, Egashira K, Mitsui T, Chishima S, Takeshita A, Narita H. Angiotensin-converting enzyme inhibitor prevents plasminogen activator inhibitor-1 expression in a rat model with cardiovascular remodeling induced by chronic inhibition of nitric oxide synthesis. *J Mol Cell Cardiol*. 2000;32:73–83.
23. Ohnishi H, Oka T, Kusachi S, Nakanishi T, Takeda K, Nakahama M, Doi M, Murakami T, Ninomiya Y, Takigawa M, Tsuji T. Increased expression of connective tissue growth factor in the infarct zone of experimentally induced myocardial infarction in rats. *J Mol Cell Cardiol*. 1998;30:2411–2422.
24. Trueblood NA, Xie Z, Communal C, Sam F, Ngoy S, Liaw L, Jenkins AW, Wang J, Sawyer DB, Bing OH, Apstein CS, Colucci WS, Singh K. Exaggerated left ventricular dilation and reduced collagen deposition after myocardial infarction in mice lacking osteopontin. *Circ Res*. 2001;88:1080–1087.
25. Rodriguez-Manzaneque JC, Lane TF, Ortega MA, Hynes RO, Lawler J, Iruela-Arispe ML. Thrombospondin-1 suppresses spontaneous tumor growth and inhibits activation of matrix metalloproteinase-9 and mobilization of vascular endothelial growth factor. *Proc Natl Acad Sci U S A*. 2001;98:12485–12490.
26. Inoki I, Shiomi T, Hashimoto G, Enomoto H, Nakamura H, Makino K, Ikeda E, Takata S, Kobayashi K, Okada Y. Connective tissue growth factor binds vascular endothelial growth factor (VEGF) and inhibits VEGF-induced angiogenesis. *FASEB J*. 2002;16:219–221.
27. Bloomston M, Shafii A, Zervos EE, Rosemurgy AS. TIMP-1 overexpression in pancreatic cancer attenuates tumor growth, decreases implantation and metastasis, and inhibits angiogenesis. *J Surg Res*. 2002;102:39–44.
28. Volpert OV, Zaichuk T, Zhou W, Reiher F, Ferguson TA, Stuart PM, Amin M, Bouck NP. Inducer-stimulated Fas targets activated endothelium for destruction by anti-angiogenic thrombospondin-1 and pigment epithelium-derived factor. *Nat Med*. 2002;8:349–357.
29. Kubasiak LA, Hernandez OM, Bishopric NH, Webster KA. Hypoxia and acidosis activate cardiac myocyte death through the Bcl-2 family protein BNIP3. *Proc Natl Acad Sci U S A*. 2002.
30. Trost SU, Omens JH, Karlon WJ, Meyer M, Mestril R, Covell JW, Dillmann WH. Protection against myocardial dysfunction after a brief

ischemic period in transgenic mice expressing inducible heat shock protein 70. *J Clin Invest*. 1998;101:855–862.
31. Hudlicka O, Brown MD. Postnatal growth of the heart and its blood vessels. *J Vasc Res*. 1996;33:266–287.
32. Dor Y, Djonov V, Abramovitch R, Itin A, Fishman GI, Carmeliet P, Goelman G, Keshet E. Conditional switching of VEGF provides new insights into adult neovascularization and pro-angiogenic therapy. *EMBO J*. 2002;21:1939–1947.
33. Osugi T, Oshima Y, Fujio Y, Funamoto M, Yamashita A, Negoro S, Kunisada K, Izumi M, Nakaoka Y, Hirota H, Okabe M, Yamauchi-Takihara K, Kawase I, Kishimoto T. Cardiac-specific activation of signal transducer and activator of transcription 3 promotes vascular formation in the heart. *J Biol Chem*. 2002;277:6676–6681.
34. Giordano FJ, Gerber HP, Williams SP, VanBruggen N, Bunting S, Ruiz-Lozano P, Gu Y, Nath AK, Huang Y, Hickey R, Dalton N, Peterson KL, Ross J, Jr., Chien KR, Ferrara N. A cardiac myocyte vascular endothelial growth factor paracrine pathway is required to maintain cardiac function. *Proc Natl Acad Sci U S A*. 2001;98:5780–5785.
35. Jimenez B, Volpert OV, Crawford SE, Febbraio M, Silverstein RL, Bouck N. Signals leading to apoptosis-dependent inhibition of neovascularization by thrombospondin-1. *Nat Med*. 2000;6:41–48.
36. Ingber DE. Mechanical signaling and the cellular response to extracellular matrix in angiogenesis and cardiovascular physiology. *Circ Res*. 2002;91:877–887.
37. Jacoby JJ, Kalinowski A, Liu MG, Zhang SS, Gao Q, Chai GX, Ji L, Iwamoto Y, Li E, Schneider M, Russell KS, Fu XY. Cardiomyocyte-restricted knockout of STAT3 results in higher sensitivity to inflammation, cardiac fibrosis, and heart failure with advanced age. *Proc Natl Acad Sci U S A*. 2003;100:12929–12934.
38. Yu Z, Zhang W, Kone BC. Signal transducers and activators of transcription 3 (STAT3) inhibits transcription of the inducible nitric oxide synthase gene by interacting with nuclear factor kappaB. *Biochem J*. 2002;367:97–105.
39. Bromberg J. Stat proteins and oncogenesis. *J Clin Invest*. 2002;109:1139–1142.
40. Kunisada K, Negoro S, Tone E, Funamoto M, Osugi T, Yamada S, Okabe M, Kishimoto T, Yamauchi-Takihara K. Signal transducer and activator of transcription 3 in the heart transduces not only a hypertrophic signal but a protective signal against doxorubicin-induced cardiomyopathy. *Proc Natl Acad Sci U S A*. 2000;97:315–319.
41. Stephanou A, Latchman DS. Transcriptional regulation of the heat shock protein genes by STAT family transcription factors. *Gene Expression*. 1999;7:311–319.

Circulation Research
JOURNAL OF THE AMERICAN HEART ASSOCIATION

Signal Transducer and Activator of Transcription 3 Is Required for Myocardial Capillary Growth, Control of Interstitial Matrix Deposition, and Heart Protection From Ischemic Injury

Denise Hilfiker-Kleiner, Andres Hilfiker, Martin Fuchs, Karol Kaminski, Arnd Schaefer, Bernhard Schieffer, Anja Hillmer, Andreas Schmiedl, Zhaoping Ding, Edith Podewski, Eva Podewski, Valeria Poli, Michael D. Schneider, Rainer Schulz, Joon-Keun Park, Kai C. Wollert and Helmut Drexler

Circ Res. 2004;95:187-195; originally published online June 10, 2004;
doi: 10.1161/01.RES.0000134921.50377.61
Circulation Research is published by the American Heart Association, 7272 Greenville Avenue, Dallas, TX 75231

Print ISSN: 0009-7330. Online ISSN: 1524-4571

STAT3 is required for Myocardial Capillary Growth, Control of Interstitial Matrix Deposition, and Protection of the Heart from Ischemic Injury

Denise Hilfiker-Kleiner[1], Andres Hilfiker[1], Martin Fuchs[1], Karol Kaminski[1], Arnd Schaefer[1], Bernhard Schieffer[1], Anja Hillmer[1], Andreas Schmiedl[2], Zhaoping Ding[3], Edith Podewski[1], Eva Podewski[1], Valeria Poli[4], Michael D. Schneider[5], Rainer Schulz[6], Joon-Keun Park[7], Kai C. Wollert[1], and Helmut Drexler[1]

[1]Departments of Cardiology and Angiology, [2]Anatomy, [7]Nephrology, Medical School Hannover, Germany; [3]Institute for Cardiovascular Physiology, University of Düsseldorf, Germany; [4]Department of Genetics, Biology, and Biochemistry, University of Turin, Italy; [5]Department of Medicine, Baylor College of Medicine, Houston, Texas, USA; [6]Department of Pathophysiology, Universitätsklinikum, Essen, Germany

Supporting Materials and Methods

Generation of Cardiomyocyte-Restricted STAT3-Deficient Mice

LoxP sites introduced in the STAT3 gene are shown in Figure 1 (online supplement). Mice were genotyped by amplification of distinctive PCR-products, using

primer a: CACCAACACATGCTATTTGTAGG, primer b: CCTGTCTCTGACAGGCCATC, primer c: GCAGCAGAATACTCTACAGCTC as illustrated in Figure 1 (online supplement) (Figure 1A in main manuscript).[1,2]

Ischemia/reperfusion

Ischemia/reperfusion (I/R)-injury was induced according to the method of Dumont.[3] Briefly, mice were anaesthetized and mechanically ventilated with enflurane (3%). After a left thoracotomy, the proximal left anterior descending coronary artery (LAD) was ligated over a

PE-10 polyethylene tube. After 1 h, blood flow was re-established by removal of the tube. Control mice underwent a sham operation (thoracotomy only).

Transthoracic echocardiography

Echocardiography was performed as described.[4] In brief, short axis M-mode images were recorded at the papillary muscle level in mice sedated with ketamine (100 mg/kg, i.p.) and xylazine (1.25 mg/kg, i.p.) using a linear 15 MHz transducer (ATL HDI 5000 CV). Fractional shortening (FS) was calculated as follows: FS [%] = [(LVEDD - LVESD) / LVEDD] x 100 (LVEDD, left ventricular end-diastolic diameter; LVESD, left ventricular end-systolic diameter).

Hemodynamics

LV hemodynamics were measured with a 1.4 F micromanometer conductance catheter (SPR-719; Millar Instruments, Houston, TX) as described.[5] In brief, mice were anaesthetized and mechanically ventilated with enflurane (3%), a bilateral vagotomy was performed, and the catheter was inserted in the LV cavity via the right carotid artery.

The right jugular vein was cannulated for infusion of dobutamine. After the catheter was in place, enflurane was reduced to 1.5% and hemodynamic stabilization was awaited. Steady-state LV pressure and conductance was sampled at a rate of 1 kHz and stored at the final 30 s of each 3-min dosage period (4 µg/kg/min up to 40 µg/kg/min, infusion time 15 min, 3 min per dose, Table 1, online supplement).

The raw conductance signal was not corrected for parallel conductance (Vp) and was not converted into real blood volume values. The conductance volume is expressed in relative volume units (RVU). The ejection fraction (EF) was computed via the formula [(stroke volume/volume at dp/dtmax) • 100] using RVU.

Metabolic Assay

The metabolic assay was performed, as described previously.[6,7] In brief, the powdered tissue samples (Mikro Dismembrator, B.Braun Melsungen, Melsungen, FRG) were extracted with

0.3 mol/L perchloric acid and neutralized with 0.9 mol/L KOH, 160 mmol/L K_2SO_4, 57 mmol/L tris. Aliquots were used for the measurements of lactate and high energy phosphates. Lactate was measured using an autoanalyzer (EML 100, Radiometer Medical A/S, Copenhagen, Denmark). High energy phosphates were measured using HPLC on an anion exchanger column (Protein Pak DEAE 5 PW, Millipore-Waters GmbH, Eschborn, FRG). The elution buffer consisted of 3 mmol/L tris/H_2SO_4 (pH 9.0) with a linear gradient from 6 to 286 mmol/L K_2SO_4 within 0 to 20 minutes of the run; the flow was 0.8 mL/min. UV absorption was monitored at 214 nm. The retention times were 10, 13, 17, 19 minutes for CP, AMP, ADP, ATP, respectively. Data are shown in Table 2 (online supplement).

Quantification of Ischemia/Reperfusion-Injury and Infarct Sizes

Area at risk and early infarct size following I/R-injury were assessed by Evan's blue and 2,3,5-triphenyltetrazolium chloride (TTC)-staining as described.[5] Infarct sizes were determined in H&E stained in *in situ* fixed (retrogradely perfused (2 min; 80 mmHg) with PBS (pH 7.4) containing 50 mM KCl and 200 U/ml heparin, followed by *in situ* paraformaldehyde-fixation) myocardial sections.[5] For quantification sections were digitalized using a planimetry system (Quantimet 500MC, Leica, Munich, Germany). Control mice underwent a sham operation (thoracotomy only).

Quantification of interstitial fibrosis with picro-Sirius red polarization method

Interstitial fibrosis was visualized in *in situ* fixed LV sections stained with picro-Sirus red using polarization filters (Axiophot, Zeiss). Sections were digitalized and collagen I and III contents were quantified using a planimetry system (Quantimet 500MC, Leica, Munich, Germany).[5]

Analysis of Apoptosis

Apoptotic nuclei were detected by *in situ* terminal deoxynucleotidyl transferase-mediated digoxigenin-conjugated dUTP nick end-labeling (TUNEL) in paraformaldehyde-fixated or frozen sections, as described.[8] Slides were counter-stained with Hoechst 33258 (Sigma) to confirm apoptotic morphology of individual nuclei. In addition, slides were double stained with

anti sarcomeric α-actinin (SIGMA). High power fields (400x, 200µmx200µm, 8 to 30 fields per section of LV basis, middle part and apex) were examined to calculate the frequency of TUNEL/Hoe positive nuclei. To confirm increased apoptosis following I/R-injury, additional LV slices were embedded in OCT and incubated with antibodies recognizing activated caspase 3 (PharMingen, polyclonal rabbit anti-active caspase-3 antibody, cat. Nr. 557053) (Figure 2, online supplement).

Capillary Density and Number of Coronary Resistance Vessels

Capillary density was determined in LV sections with transversely-sectioned cardiomyocytes immunostained against platelet-endothelial cell adhesion molecule–1 (PECAM-1) (Santa Cruz) and counterstained with hematoxylin or Hoechst 33258 (Sigma).[9] The ratio of PECAM-1 positive cells to total nuclei (Hematoxylin or Hoechst stain) was calculated. High power fields (400x, 200µmx200µm, 8 fields per section of LV basis, middle part and apex, n=4 per genotype) with transversely sectioned cardiomyocytes were digitally recorded (Quantimet 500MC). Capillary-to-cardiomyocyte ratio was measured in van Gieson stained *in situ* fixated transverse sections or in frozen sections double stained for PECAM-1 and WGA. For each mouse high power fields (400x, 200µmx200µm, 8 fields per section of LV basis, middle part and apex) with transversely sectioned cardiomyocytes were digitally recorded to calculate capillary to cardiomyocyte ratio.

Coronary resistance vessels were counted in *in situ* fixed H&E stained transvers LV sections (three sections per heart, basis, middle part and apex, all resistance vessels per section were counted, n=4 for each genotype). We distinguished vessels with diameters from 25µm to 50µm separately from those with diameters of 50µm to 150µm. For small vessels (25µm to 50µm) we counted an average of 165±36 in WT and 155±49 in KO; for larger vessels (50µm to 150µm), we counted 64±10 in WT and 64±14 in KO.

Investigator were blinded for caplillary density and coronary density quantification.

Isolation and cultivation of mouse lung endothelial cells, proliferation assays with ^{3}H-Thymidin incorporation

Mouse lungs were digested with Type I collagenase (2mg/ml, Worthington) in DMEM supplemented with 20% FCS. Endothelial cells were isolated using the OctoMACS Starting Kit (Miltenyi Biotec GmbH) by selecting PECAM-1 (BD) positive cells in a first purification step and seeded on fibronectin coated plates. In a second purification step cells were collected from plates and ICAM-2 (BD) positive cells were selected with OctoMACS, seeded on fibronectin coated plates and maintained in DMEM supplemented with 20% FCS. A small fraction of cells were seeded in fibronectin coated chamber slides and stained with PECAM-1 antibody to verify endothelial cell type. Cells were serum deprived for 24 h before exposure to cardiomyocyte supernatant.

Proliferation assays with 3^{H}-Thymidin incorporation (performed in triplicates) were performed with cardiomyocyte supernatant from n=4 individual cell preparations.

cDNA and Oligonucleotide-Probes for Northern-blotting

cDNA probes for VEGF, BNIP3 and TIMP1 generated by RT-PCR cloning using mouse specific primer pairs shown below. cDNA probes for atrial natriuretic peptide (ANP),[10] glyceraldehyde-3-phosphate dehydrogenase (G3PDH),[11] and sarco(endo)plasmic reticulum Ca^{2+}-ATPase-2a (SERCA2a), have been described previously.[11] Probes were [^{32}P]-labeled by random priming. Oligonucleotides specific for αMHC and βMHC were end-labeled with [^{32}P].[12] Loading and transfer efficiency were controlled by densiometric analysis of etidium bromide stained 18S rRNA.

RT-PCR Primer Sequences

BCL-2: CCAACTCCCGATTCATTG / AGTCACGACGGTAGCGAC

BCL-X: CCCCAGTGCCATCAATG / GTGAGTGGACGGTCAGTGTC

BNIP3: CCCTGCTACCTCTCGGTG / AAAGTGGGGTTCGTGGG

CTGF: CCCGAGAAGGGTCAAGC / ATGTTTTCCTCCAGGTCAGC

G3PDH:	ACCACCATGGAGAAGGCTGG / CTCAGTGTAGCCCAGGATGC
PlGF:	CTGAGTCGCTGTAGTGGC / CACGAAGACACACAACCC
PTGFR:	AAACTTGCCAGTCGTTGC / CATTGTATCTGTCTATCTCCTGTTG
TIMP1:	AGATGCTAAAAGGATTCAAGGC / CGTCCACAAACAGTGAGTGTC
TNC:	CCCCCGAACGTACCAGG / TTTATGCCCGCTTACGCC
TSP1:	GCTTTTCATCTGGGGCTCAC / ATCTCTATTCCAATGGCAACGAG
VEGF:	TACCAGCGAAGCTACTGCC / GACCCAAAGTGCTCCTCG
HSP 70:	AGCAGACGCAGACCTTCAC / AACCTTGACAGTAATCGGTGC

References

1. Alonzi T, Maritano D, Gorgoni B, Rizzuto G, Libert C, Poli V. Essential role of STAT3 in the control of the acute-phase response as revealed by inducible gene inactivation [correction of activation] in the liver. *Mol Cell Biol*. 2001;21:1621-32.
2. Gaussin V, Van de Putte T, Mishina Y, Hanks MC, Zwijsen A, Huylebroeck D, Behringer RR, Schneider MD. Endocardial cushion and myocardial defects after cardiac myocyte-specific conditional deletion of the bone morphogenetic protein receptor ALK3. *Proc Natl Acad Sci U S A*. 2002;99:2878-83.
3. Dumont EA, Hofstra L, van Heerde WL, van den Eijnde S, Doevendans PA, DeMuinck E, Daemen MA, Smits JF, Frederik P, Wellens HJ, Daemen MJ, Reutelingsperger CP. Cardiomyocyte death induced by myocardial ischemia and reperfusion: measurement with recombinant human annexin-V in a mouse model. *Circulation*. 2000;102:1564-8.
4. Schaefer A, Klein G, Brand B, Lippolt P, Drexler H, Meyer GP. Evaluation of left ventricular diastolic function by pulsed Doppler tissue imaging in mice. *J Am Soc Echocardiogr*. 2003;16:1144-9.
5. Fuchs M, Hilfiker A, Kaminski K, Hilfiker-Kleiner D, Guener Z, Klein G, Podewski E, Schieffer B, Rose-John S, Drexler H. Role of interleukin-6 for left ventricular remodeling and survival after experimental myocardial infarction. *Faseb J*. 2003.
6. Martin C, Schulz R, Rose J, Heusch G. Inorganic phosphate content and free energy change of ATP hydrolysis in regional short-term hibernating myocardium. *Cardiovasc Res*. 1998;39:318-26.
7. Martin C, Schulz R, Post H, Gres P, Heusch G. Effect of NO synthase inhibition on myocardial metabolism during moderate ischemia. *Am J Physiol Heart Circ Physiol*. 2003;284:H2320-4.
8. Wollert KC, Heineke J, Westermann J, Ludde M, Fiedler B, Zierhut W, Laurent D, Bauer MK, Schulze-Osthoff K, Drexler H. The cardiac Fas (APO-1/CD95) Receptor/Fas ligand system : relation to diastolic wall stress in volume-overload

hypertrophy in vivo and activation of the transcription factor AP-1 in cardiac myocytes. *Circulation*. 2000;101:1172-8.

9. Scherrer-Crosbie M, Ullrich R, Bloch KD, Nakajima H, Nasseri B, Aretz HT, Lindsey ML, Vancon AC, Huang PL, Lee RT, Zapol WM, Picard MH. Endothelial nitric oxide synthase limits left ventricular remodeling after myocardial infarction in mice. *Circulation*. 2001;104:1286-91.

10. Wollert KC, Taga T, Saito M, Narazaki M, Kishimoto T, Glembotski CC, Vernallis AB, Heath JK, Pennica D, Wood WI, Chien KR. Cardiotrophin-1 activates a distinct form of cardiac muscle cell hypertrophy. Assembly of sarcomeric units in series VIA gp130/leukemia inhibitory factor receptor-dependent pathways. *J Biol Chem*. 1996;271:9535-45.

11. Hasenfuss G, Reinecke H, Studer R, Meyer M, Pieske B, Holtz J, Holubarsch C, Posival H, Just H, Drexler H. Relation between myocardial function and expression of sarcoplasmic reticulum Ca(2+)-ATPase in failing and nonfailing human myocardium. *Circ Res*. 1994;75:434-42.

12. Zhang X, Azhar G, Chai J, Sheridan P, Nagano K, Brown T, Yang J, Khrapko K, Borras AM, Lawitts J, Misra RP, Wei JY. Cardiomyopathy in transgenic mice with cardiac-specific overexpression of serum response factor. *Am J Physiol Heart Circ Physiol*. 2001;280:H1782-92.

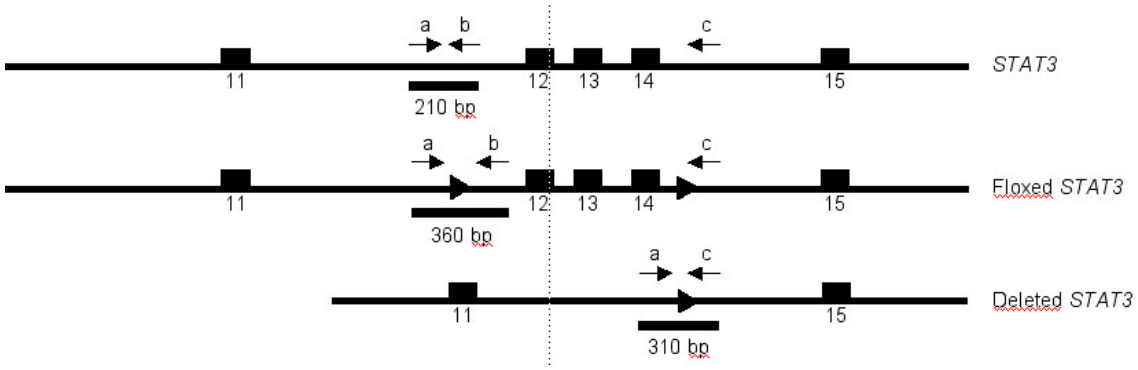

Figure 1/online supplement. Genomic structure (exons 11 through 15) of *STAT3*, floxed *STAT3*, and deleted *STAT3* alleles. PCR primers a, b, and c, used for genotyping are shown.

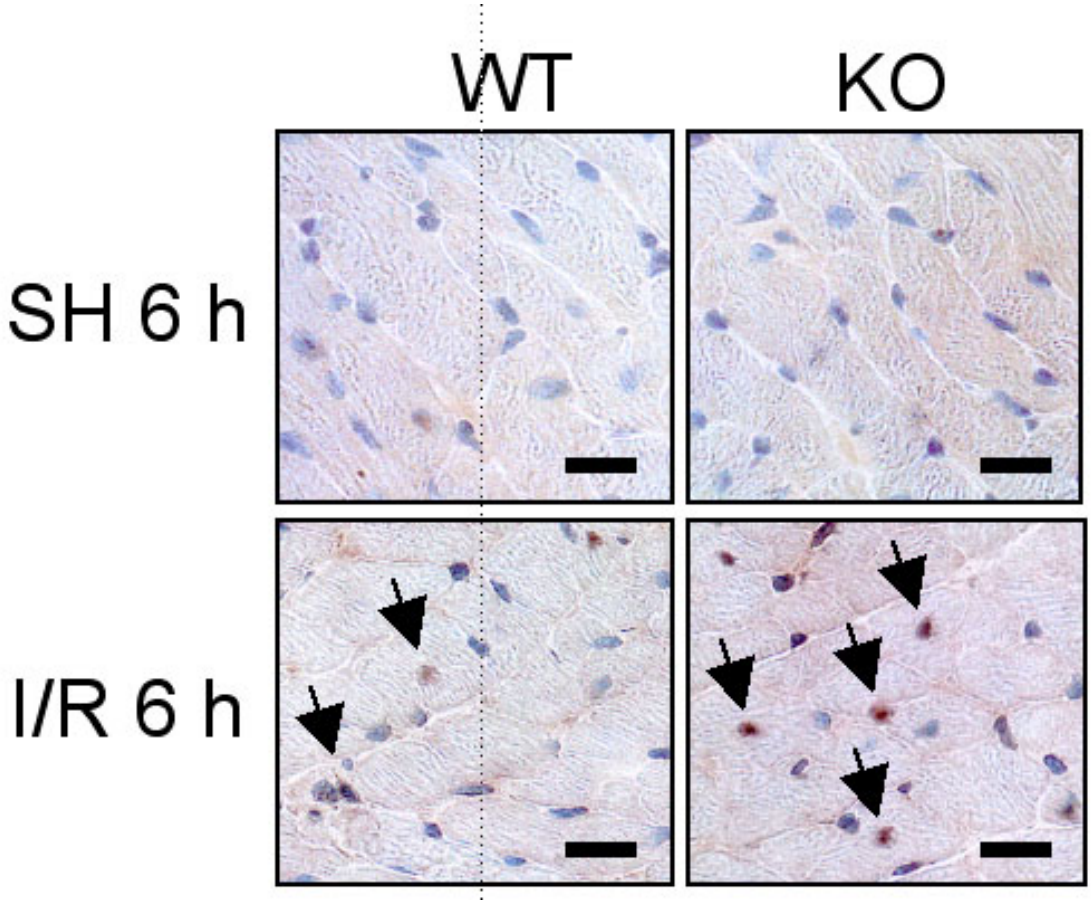

Figure 2/online supplement. Increased susceptibility to apoptosis in response to I/R-injury in STAT3 KO mice. Increased number of activated caspase 3-positive nuclei (arrows)

following 1 h of ischemia and 6 h of reperfusion in a representative LV section from a 3 month-old KO mouse as compared to a WT mouse.

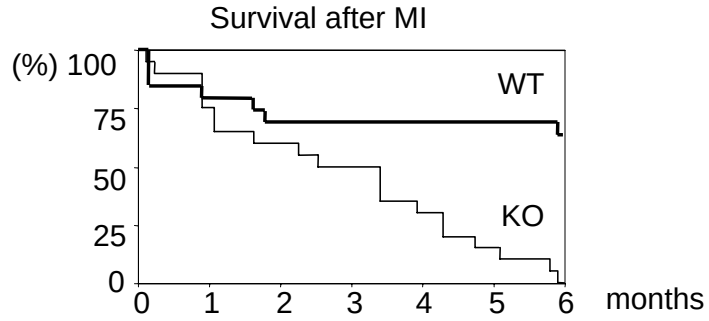

Figure 3/online supplement. Kaplan-Meier curves depicting survival of WT (n=19) and KO (n=21) mice following infarction (*P*<0.01 log-rank test).

Table 1/online supplement

Hemodynamic Parameters in WT and KO mice basal and exposed to dobutamine

	HR	End-systolic. Pressure	End-diastolic. Pressure	EF (%)	dP/dt (max)	dP/dt (min)
WT basal	509±20	111±8.4	0.88±4.86	14.4±3.8	6374±1976	-5268±1326
KO basal	442±40*	99±16	9.68±13.0	13.4±5.2	5848±1234	-5996±1470
WT dobutamine	565±18	92±14	-5.3±7.2	18.3±5.5	8034±509	-5947±1154
KO dobutamine	506±17**	91±24	-1.34±4.5	12.1±4.3	6663±1075	-5497±796

HR, heart rate in beats per minute; end-systolic and end-diastolic pressure in mmHg; dP/dt (max) in mmHg/sec; dP/dt (min) in mmHg/sec. Dobutamine infusion (40 µg/kg/min). *P<0.05, **P<0.01 vs corresponding WT.

Table 2/online supplement

Metabolic assay

	CP (µMol/g)	AMP (µMol/g)	ADP (µMol/g)	ATP (µMol/g)	Lactate (µMol/g)
WT (n=5)	0.55±0.21	0.37±0.13	1.07±0.16	1.02±0.14	3.43±1.30
KO (n=4)	0.55±043	0.5±0.25	1.17±0.20	0.87±0.18	5.58±0.74*

All mice were exposed to dobutamine infusion (40 µg/kg/min). CP, creatine phosphate; *P<0.05.

Table 3/online supplement

cDNA Microarray analysis – extended data set

cDNA-probes, derived from left ventricles of 3-4 month-old STAT3 KO and WT mice (n=5 each), were hybridized to custom-made cDNA-microarrays containing 648 genes. Genes differentially expressed by more then 1.5 fold in KO vs WT are listed below. Genes differing in their expression levels by more than ±1.8 fold are also shown in Figure 3B of the main manuscript.

Gene name	SwissProt	Unigene	
STAT3:SIGNAL TRANSDUCER AND ACTIVATOR OF TRANSCRIPTION 3	P42227	Mm.3948	-3.85
PTGFR: PROSTAGLANDIN F2 ALPHA RECEPTOR	P43117	Mm.4170	-2.63
PRKCE: PROTEIN KINASE C, EPSILON	P16054	Mm.12808	-1.96
BM3B:BONE MORPHOGENETIC PROTEIN 3B	P97737	Mm.40323	-1.82
NRF3: NFE2-RELATED FACTOR 3	Q9WTM4	Mm.42138	-1.82
ASB-4: ANKYRIN REPEAT-CONTAINING PROTEIN ASB-4	Q9WV71	Mm.181825	-1.72
IQGAP2: (IQGAP2) RASGAP-RELATED PROTEIN.			-1.59
PLGF: PLACENTA GROWTH FACTOR	P49764	Mm.4809	-1.56
ASC: APOPTOSIS-ASSOCIATED SPECK-LIKE PROTEIN	Q9EPB4	Mm.24163	-1.54
CD28	P31041	Mm.1060	-1.52
CCL6: SMALL INDUCIBLE CYTOKINE A6	P27784	Mm.137	1.54
FCGR2_MOUSE: IGG FC RECEPTOR II BETA	P97917	Mm.10809	1.57
SPARC: SPARC	P07214	Mm.35439	1.59
PYK2: FOCAL ADHESION KINASE 2	Q9QVP9		1.65
MMP3:STROMELYSIN-1	P28862	Mm.4993	1.66
FIBRILLIN1	Q61554	Mm.735	1.66
COL1A1:COLLAGEN ALPHA 1(I)	P11087	Mm.22621	1.66
MATRIXGLA:	P19788	Mm.87793	1.74
COL1A2: COLLAGEN ALPHA 2(I) CHAIN PRECURSOR.	Q01149	Mm.4482	1.82
CD72: B-CELL DIFFERENTIATION ANTIGEN CD72 (LYB-2).	P21855	Mm.88200	1.83
BGN: BIGLYCAN	P28653	Mm.2608	1.85
CTGF: CONNECTIVE TISSUE GROWTH FACTOR	P29268	Mm.1810	1.86

CD74: HLA CLASS II HISTOCOMPATIBILITY ANTIGE	P04441	Mm.7043	1.86
TSP-1: THROMBOSPONDIN1	P35441	Mm.138425	1.88
CD52: CAMPATH-1 ANTIGEN	Q64389	Mm.24130	1.89
FRE: FRIZZLED-RELATED PROTEIN	P97401	Mm.3246	1.90
COL8A1: COLLAGEN ALPHA 1(VIII)	Q00780	Mm.86813	1.94
BCL2A1: BCL2-RELATED PROTEIN A1	Q07440	Mm.87855	2.06
PAI1: PLASMINOGEN ACTIVATOR INHIBITOR-1 PRECURSOR	P22777	Mm.1263	2.07
OPN: OSTEOPONTIN	P10923	Mm.321	2.16
CDKN1A: CYCLIN-DEPENDENT KINASE INHIBITOR 1	P39689	Mm.34446	2.30
MCP3: CCL7, SMALL INDUCIBLE CYTOKINE A7 PRECURSOR	Q03366	Mm.16091	2.61
IL2RB: INTERLEUKIN-2 RECEPTOR BETA	P16297	Mm.931	2.99
TNC: TENASCINC	Q64706	Mm.980	3.10
IL15: INTERLEUKIN-15	P48346	Mm.4392	3.35
MCP1: CCL2, SMALL INDUCIBLE CYTOKINE A2, MCP1	P10148	Mm.145	3.89
MMP12: MACROPHAGE METALLOELASTASE	P34960	Mm.2055	4.24
TIMP1: METALLOPROTEINASE INHIBITOR 1	P12032	Mm.8245	5.90